Annals of Biomedical Engineering, Vol. 40, No. 4, April 2012 (© 2011) pp. 946–954
DOI: 10.1007/s10439-011-0460-9

BMES BIOMEDICAL ENGINEERING SOCIETY™ www.bmes.org

A Novel Frequency Analysis Method for Assessing $K_{ir}2.1$ and $Na_v1.5$ Currents

J. R. RIGBY[1,2] and S. POELZING[1,2]

[1]Nora Eccles Harrison Cardiovascular Research and Training Institute, University of Utah, 95 South 2000 East, Salt Lake City, UT 84112, USA; and [2]Department of Bioengineering, University of Utah, 72 South Central Campus Drive, Room 2750, Salt Lake City, UT 84112, USA

(*Received 26 July 2011; accepted 28 October 2011; published online 4 November 2011*)

Associate Editor Ioannis A. Kakadiaris oversaw the review of this article.

Abstract—Voltage clamping is an important tool for measuring individual currents from an electrically active cell. However, it is difficult to isolate individual currents without pharmacological or voltage inhibition. Herein, we present a technique that involves inserting a noise function into a standard voltage step protocol, which allows one to characterize the unique frequency response of an ion channel at different step potentials. Specifically, we compute the fast Fourier transform for a family of current traces at different step potentials for the inward rectifying potassium channel, $K_{ir}2.1$, and the channel encoding the cardiac fast sodium current, $Na_v1.5$. Each individual frequency magnitude, as a function of voltage step, is correlated to the peak current produced by each channel. The correlation coefficient vs. frequency relationship reveals that these two channels are associated with some unique frequencies with high absolute correlation. The individual IV relationship can then be recreated using only the unique frequencies with magnitudes of high absolute correlation. Thus, this study demonstrates that ion channels may exhibit unique frequency responses.

Keywords—Whole-cell voltage clamp, Impedance spectroscopy, Ion channel, Frequency response.

INTRODUCTION

Voltage clamp techniques are among an electrophysiologist's principle tools with which to study various properties of ion channels such as activation and inactivation kinetics and their voltage dependence.[10] In the whole-cell configuration, the measured current is a sum of ion fluxes through all channels in the membrane. When multiple channel types are present, current through the channel type of interest can be isolated by either pharmacologically blocking other channel types or by using a voltage protocol that would cause non-desired channels to inactivate.[1,9,14] However, pharmacological agents often have non-specific interactions, and voltage-inactivation is not always possible.

Furthermore, it is difficult to distinguish individual ion channel types from an amalgamated current. The most common solution is to measure a specific ionic current as the difference in total current measured before and after application of a supra maximal dose of a drug that blocks the channel.[21] One limitation of this approach is that it cannot elucidate interrelationships between different ionic currents. For example, if one channel modulates the function of another, the sum of their individual current contributions measured separately may not be equivalent to the total current from both channels measured simultaneously. Again, this technique is not always feasible since many widely used drugs have non-specific interactions.[14,29]

Heterologous expression systems have been very powerful and useful tools for studying many aspects of ion channels since they allow a single channel type to be isolated, but they too suffer from the limitations already mentioned when the goal is to study the interrelation of multiple channels.[28]

One way to address this limitation may be to use frequency information from the impedance of individual channel types. It has been shown that blocking potassium or calcium channels in chromaffin cells increases the impedance of the cell in a frequency-dependent manner.[11] Numerous studies have used impedance spectroscopy to characterize various ion channels expressed in both artificial lipid bilayers and various biological preparations.[11–13,18,19] However, it

Address correspondence to S. Poelzing, Nora Eccles Harrison Cardiovascular Research and Training Institute, University of Utah, 95 South 2000 East, Salt Lake City, UT 84112, USA. Electronic mail: poelzing@cvrti.utah.edu

remains unknown whether impedance spectra are uniquely associated with different channel types. We hypothesized that ion channels conducting distinctly different ions will exhibit unique frequency responses and that frequency magnitude information from each channel can be used to reproduce properties of the macroscopic currents when measured separately.

METHODS

Current Recordings in HEK293 Cells

$K_{ir}2.1$ currents were recorded from HEK293 cells stably transfected with the KCNJ2 gene (kind gift of Dr. Min Li, John Hopkins University). Acquisition and use of this cell line is in accordance with the University of Utah's policy on cell use. $Na_v1.5$ currents were recorded from HEK293 cells transiently transfected with the SCN5A gene using Lipofectamine 2000 (Invitrogen, Carlsbad, CA) according to the manufacturer's instructions. All voltage clamp experiments were performed in the whole-cell configuration using an Axopatch-200 amplifier (Molecular Devices, Sunnyvale, CA). Command potentials and data acquisition were controlled using pClamp 8.0 software (Molecular Devices). Internal and bath solutions were prepared as previously published.[22,24] Microelectrodes with a resistance of 1–2 MΩ were made from borosilicate capillary glass (WPI, Sarasota, FL). To control for the possibility of interference from endogenously expressed ion channels or artifacts generated by the system hardware, ionic current flux through $K_{ir}2.1$ channels was blocked by adding 300 μM $BaCl_2$ to the bath solution drop wise until complete functional block was observed.[20] The anti-aliasing lowpass filter on the amplifier was set to the highest available cutoff frequency (50 kHz), and the sampling frequency was set to 200 kHz for $K_{ir}2.1$ and 500 kHz for $Na_v1.5$.

Stimulus Files and Noise Function

Stimulus files were generated using custom software created in Matlab (The MathWorks, Natick, MA) and were used to define the command potential at each time step. Voltage step protocols had a holding potential of −90 mV, and stepped from −133 to −14 mV in 7 mV steps for $K_{ir}2.1$ or −84 to +63 mV in 7 mV steps for $Na_v1.5$. Each voltage step contained either a 30 ms noise function that began 100 ms after the beginning of the step ($K_{ir}2.1$), or a 2 ms noise function that began 0.24 ms after the beginning of the step ($Na_v1.5$). Analogous stimulus files were also created without a noise function for making control measurements. Graphical representations of the voltage step protocols encoded by the stimulus files can be seen as insets in Figs. 1a and 4a for $K_{ir}2.1$ and $Na_v1.5$, respectively. The noise functions were created using Matlab by first defining a square wave in the frequency domain containing equal magnitudes of all frequencies from 1 to 15 kHz, then computing the inverse fast Fourier transform (IFFT) of the signal, and finally scaling the signal in the time domain so as to make the zero to peak amplitude 100 mV.

Data Analysis

Custom software written in Matlab was used for all data analysis. $K_{ir}2.1$ and $Na_v1.5$ recordings were analyzed identically in all respects. The fast Fourier transform (FFT) was computed for the portion of all current recordings containing the noise function. For each frequency, the magnitude of that frequency at all step potentials were concatenated and correlated with the steady state current amplitude at the same transmembrane potentials. Frequencies of interest were defined as those with correlation coefficients (R) equal to 0 or $|R|$ greater than 0.8. Frequencies with absolute correlation coefficients greater than 0.8 represent frequencies whose magnitudes can be used to recreate the DC component of the ionic current. Similarly, frequencies with correlation coefficients equal to zero (termed 'zero crossings') represent frequencies whose magnitudes are independent of the ionic current. The frequencies where zero crossings occurred were quantified and compared to frequencies that had a magnitude of zero to determine which, if any frequencies, may have had no correlation because there was no power in that frequency.

Summary data are presented as mean ± standard deviation. Values were deemed to be significantly different if the p value of a student's t test was <0.05. Frequencies used for recreating the IV relationships of the channels were selected by calculating the mean of a contiguous group of frequencies exceeding a correlation coefficient of 0.8 and denoting this as the center frequency. The center frequencies for $K_{ir}2.1$ and $Na_v1.5$ were 4.0 and 25.5 kHz, respectively. The mean magnitude of the 30 ($K_{ir}2.1$) or 5 ($Na_v1.5$) frequencies surrounding this center frequency were then averaged. Finally, IV relationships were recreated from frequency magnitudes by normalizing the frequency magnitude at each voltage step to the maximum and minimum current of the IV relationship.

RESULTS

$K_{ir}2.1$—Control

Ionic currents were measured from HEK293 cells expressing $K_{ir}2.1$ during a standard voltage step

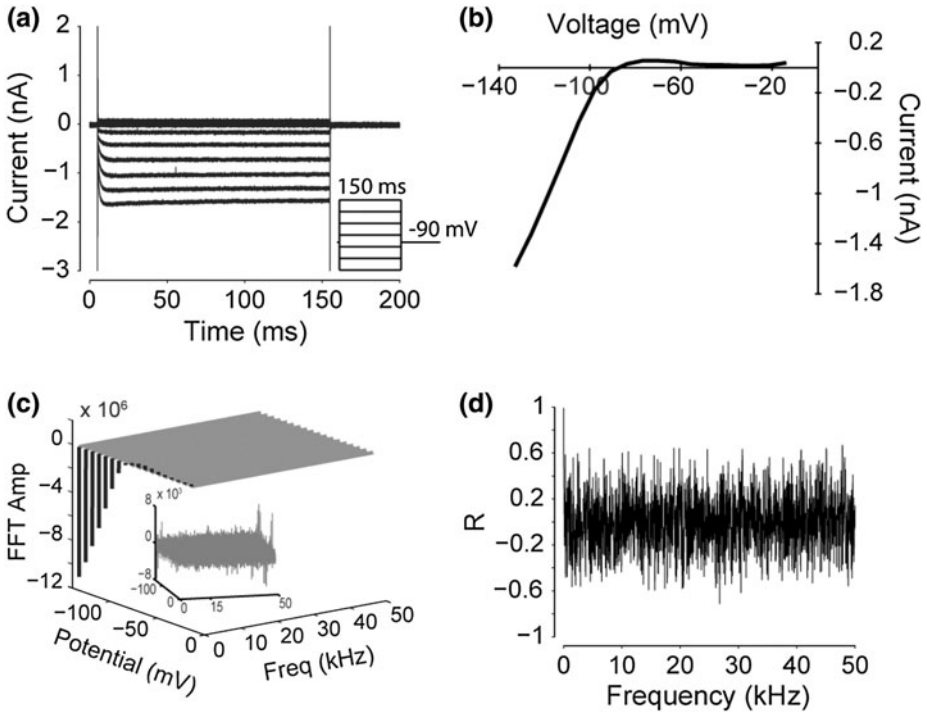

FIGURE 1. (a) Representative $K_{ir}2.1$ current in response to voltage step protocol. (b) Representative IV relationship under control conditions. (c) Representative FFT of a 30 ms portion of each voltage step. Inset is same as main panel, except DC component is removed and remaining frequencies are full scaled. (d) Representative correlation–frequency plot comparing the IV relationship to the magnitude of individual frequencies in the FFT (repeated in $n = 6$ cells).

protocol. Representative $K_{ir}2.1$ ionic currents in response to 18 voltage steps (control) are shown in Fig. 1a. An IV relationship was generated for each cell and served as the paired control IV relationship in individual cells (Fig. 1b). The FFT of all 18 voltage steps were calculated over a steady state range of the current trace ($t = 105$–135 ms), and a representative FFT magnitude, step potential, and frequency plot was generated as seen in Fig. 1c. As expected, the magnitude of the lowest frequency in each spectrum appears to mimic the shape of an IV relationship generated from Kir2.1. Specifically, the magnitude of the 0 kHz frequency (DC) decreases from −150 to −90 mV, consistent with a decrease in $K_{ir}2.1$ current amplitude over this same voltage range. In Fig. 1c (inset), the DC magnitude was removed. The non-DC frequency magnitudes were three orders of magnitude smaller than the DC magnitude (Fig. 1c, inset) and exhibited no visible pattern between step potentials.

The magnitude of every frequency as a function of step potential was then correlated to the paired control IV relationship. Figure 1d contains a representative plot of correlation coefficients for each frequency magnitude. Importantly, the correlation coefficient for the DC signal was greater than 0.99 ($p < 0.001$), verifying the visual observation that the DC magnitude mimics the shape of the IV relationship. Also note that DC is the only frequency which has an absolute correlation coefficient greater than 0.8, which we define to be the range of significant correlation.

$K_{ir}2.1$—Noise Function

$K_{ir}2.1$ ionic currents were measured with a 30 ms white-noise function added to the voltage step protocol as can be seen in Fig. 2a. The noise function contained equal magnitudes of all frequencies from 1 to 15 kHz and was inserted at the same time points used for analysis of the control recordings. The corresponding IV relationship for the recording in Fig. 2a is plotted in Fig. 2b (solid line). The FFT was calculated for the portion of each sweep containing the noise function, just as was done in the control recordings. Upon addition of the noise function, the magnitude of the DC frequency was still higher than other magnitudes (Fig. 2c). However, when the DC component was removed, frequencies up to 15 kHz exhibited a visually discernable pattern between step potentials (Fig. 2c, inset).

The magnitude of the DC component over all voltage steps correlated highly with the $K_{ir}2.1$ IV relationship obtained from the paired no-noise recording for a representative experiment (Fig. 2d). Importantly, two other frequency ranges also exceeded

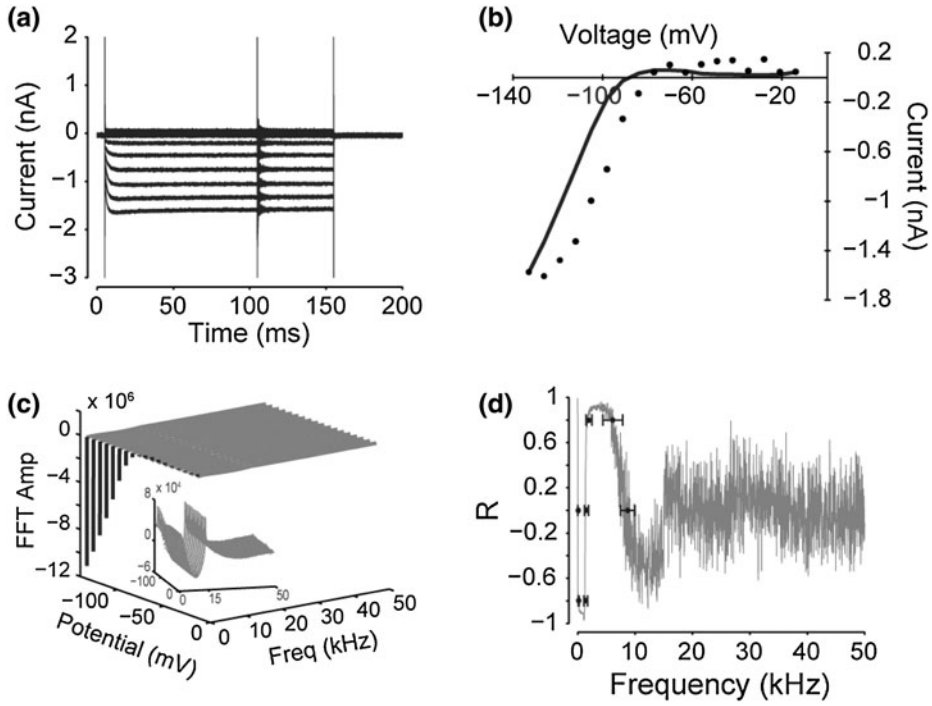

FIGURE 2. (a) Representative $K_{ir}2.1$ current in response to voltage step protocol with inserted noise function. (b) Representative $K_{ir}2.1$ IV relationship generated using current amplitudes (solid line) and the mean of all frequency magnitudes from all experiments between 3.5 and 4.5 kHz (solid circles). (c) Representative FFT of a 30 ms portion of each voltage step taken from the time points where the noise function was inserted. Inset is same as main panel, except DC component is removed and remaining frequencies are full scaled. (d) Representative correlation–frequency plot comparing the IV relationship to the magnitude of individual frequencies in the FFT. Mean and standard deviation of summary data for all experiments is plotted as filled circles with bars (repeated in $n = 6$ cells).

an absolute correlation coefficient of 0.8 (Fig. 2d). Over all experiments, frequencies between 0.17 ± 0.02 and 1.393 ± 0.004 kHz exhibited correlation coefficients below -0.8, and these values were significantly different from each other (Fig. 2d). Summary data is plotted as solid circles with standard deviation bars in Fig. 2d. Additionally, frequencies between 1.969 ± 0.202 and 6.035 ± 0.674 kHz exhibited correlation coefficients above 0.8, and these values were significantly different from each other. Frequency magnitudes of 0.045 ± 0.003 1.528 ± 0.039, and 8.737 ± 0.510 kHz exhibited zero correlation with the $K_{ir}2.1$ IV relationship.

The mean magnitude of frequencies between 3.5 and 4.5 kHz for each voltage step is overlaid on the paired IV relationship in Fig. 2b as solid circles. Magnitudes for frequencies in this range exhibited high positive correlation with the $K_{ir}2.1$ IV relationship, and visual inspection confirms similar morphologies between the IV relationship and the magnitudes of these frequencies.

$K_{ir}2.1$—Noise Function + $BaCl_2$

To test for the possibility that correlations might have been a system artifact or due to endogenous current, $K_{ir}2.1$ currents were measured with the noise function after $K_{ir}2.1$ inhibition with $BaCl_2$ (Fig. 3a). The IV relationship after current blockade with $BaCl_2$ is shown in Fig. 3b. In Fig. 3c, DC magnitudes are reduced relative to the no noise (Fig. 1c) and noise (Fig. 2c) case. Additionally, non-DC frequencies still exhibited a visually discernable pattern between voltage steps similar to the noise case. Correlation coefficients for DC magnitudes and the $K_{ir}2.1$ IV relationship still exceeded 0.8. However, all other frequencies demonstrated low correlation with the IV relationship (Fig. 3d).

$Na_v1.5$—Control

A similar experimental protocol was applied to HEK293 cells transfected with $Na_v1.5$. Representative current traces (Fig. 4a), IV relationship (Fig. 4b), FFT (Fig. 4c), and correlation spectrum (Fig. 4d) for $Na_v1.5$ under control conditions are presented in the same manner as $K_{ir}2.1$. The magnitude of the 0 Hz frequency (Fig. 4c) appeared to mimic the shape of the IV relationship (Fig. 4b) and this was confirmed by high correlation in the DC range (Fig. 4d).

Additionally, there does not appear to be a visually discernable pattern between voltage steps for frequencies above 0 Hz. Interestingly, the correlation

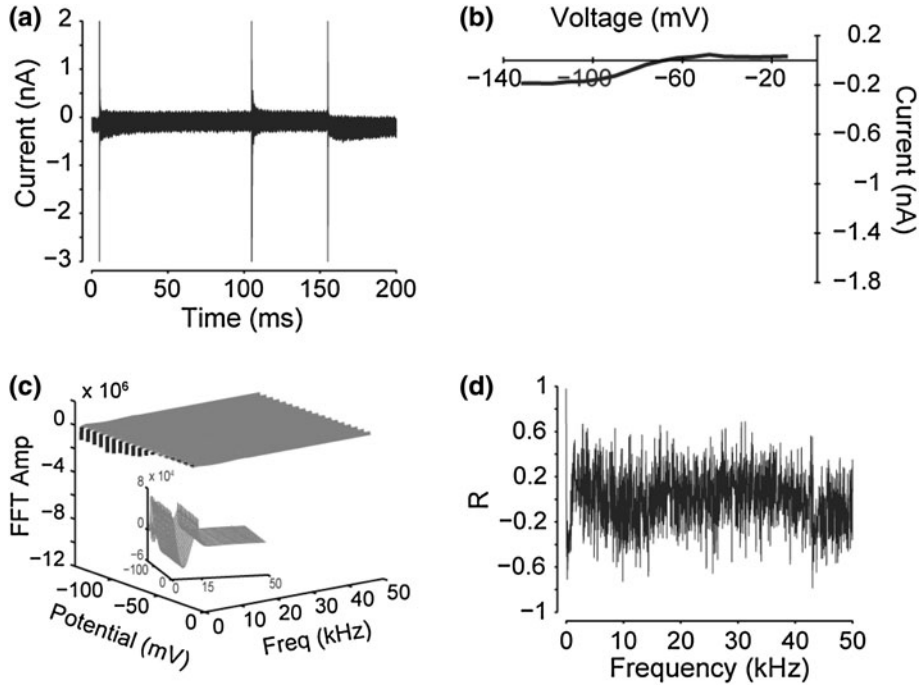

FIGURE 3. (a) Representative $K_{ir}2.1$ current and representative IV relationship (b) with noise function inserted and supramaximal dose of $BaCl_2$ added to block Kir2.1. (c) Representative FFT of a 30 ms portion of each voltage step taken from the time points where the noise function was inserted. Inset is same as main panel, except DC component is removed and remaining frequencies are full scaled. (d) Representative correlation–frequency plot comparing the IV relationship to the magnitude of individual frequencies in the FFT (repeated in $n = 3$ cells).

spectrum (Fig. 4d) demonstrated that some frequency magnitudes below 10 kHz modestly correlated with the IV relationship. However, none of the correlation coefficients exceeded an absolute value of 0.8, the correlation threshold considered significant in this study. Correlation coefficients beyond 10 kHz did not exceed 0.5.

$Na_v1.5$—Noise Function

$Na_v1.5$ ionic currents were measured with a 2 ms white-noise function (1–15 kHz) added to the voltage step protocol as can be seen in Fig. 5a, along with the paired control IV relationship in Fig. 5b. The noise function was inserted 0.24 ms after the change to the step potential. The FFT was calculated as previously described for the portion of each sweep containing the noise function. Upon addition of the noise function, frequencies from 0 to 15 kHz exhibited a consistent pattern between step potentials similar to representative data plotted in Fig. 5c.

Importantly, the correlation coefficient spectrum confirmed high DC correlation (Fig. 5d), as in all previous experiments. In this representative correlation spectrum, it is worth noting that there are frequency ranges with absolute correlations exceeding 0.8 both within the frequency of inserted noise (0–15 kHz) and beyond (>15 kHz). For all experiments (Fig. 5d, solid circles), frequency magnitudes between 3.147 ± 1.024 and 5.938 ± 0.614 kHz exceed the negative correlation threshold of -0.8, frequency magnitudes between 22.473 ± 0.570 and 28.829 ± 1.989 kHz exceeded the positive correlation threshold of 0.8, and frequency magnitudes of 1.051 ± 0.261, 8.371 ± 1.713, and 31.858 ± 1.890 kHz exhibited no correlation with the Nav1.5 IV relationship. Additional frequency magnitude correlations beyond 35 kHz were not quantified.

The mean magnitude of frequencies between 24.5 and 26.5 kHz (solid circles) for each voltage step is overlaid on the paired IV relationship in Fig. 5b. Magnitudes for frequencies in this range exhibited high positive correlation with the $Na_v1.5$ IV relationship, and visual inspection confirms similar morphologies between the IV relationship and the magnitude of these frequencies.

Zero Crossings: FFT and Correlation Coefficients

As can be seen in the insets of Figs. 1c, 2c, and 3c, the magnitude of frequencies cross zero. It was therefore important to determine whether points of zero correlation were a result of a lack of power in the frequency spectrum. To test this, frequencies with a mean magnitude equal to zero for every experiment

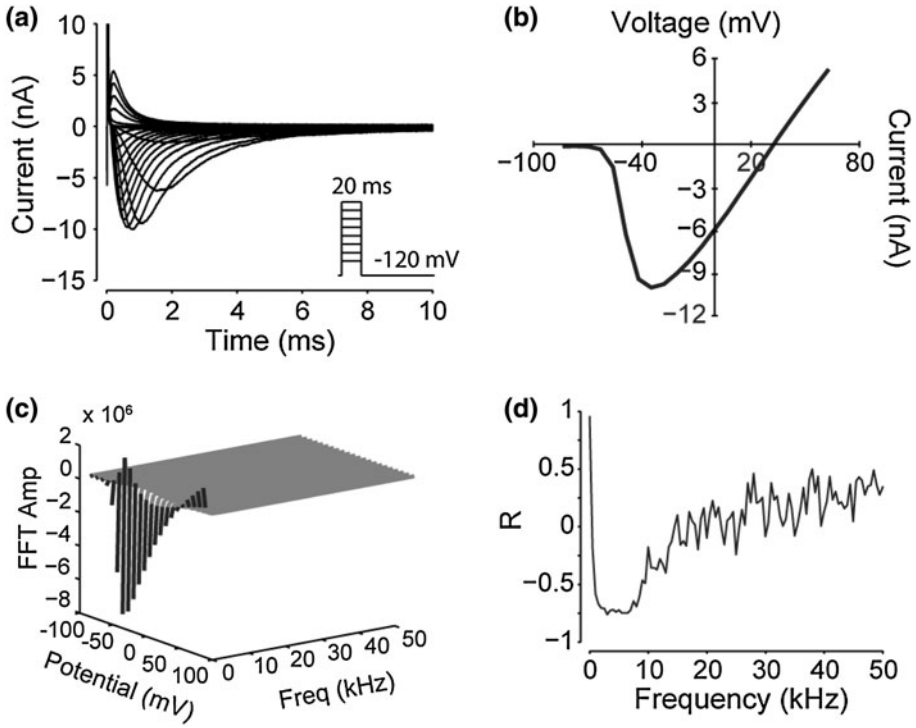

FIGURE 4. (a) Representative $Na_v1.5$ current in response to a voltage step protocol. (b) Representative IV relationship under control conditions. (c) Representative FFT of a 2 ms portion of each voltage step. (d) Representative correlation–frequency plot comparing the IV relationship to the magnitude of individual frequencies in the FFT (repeated in $n = 3$ cells).

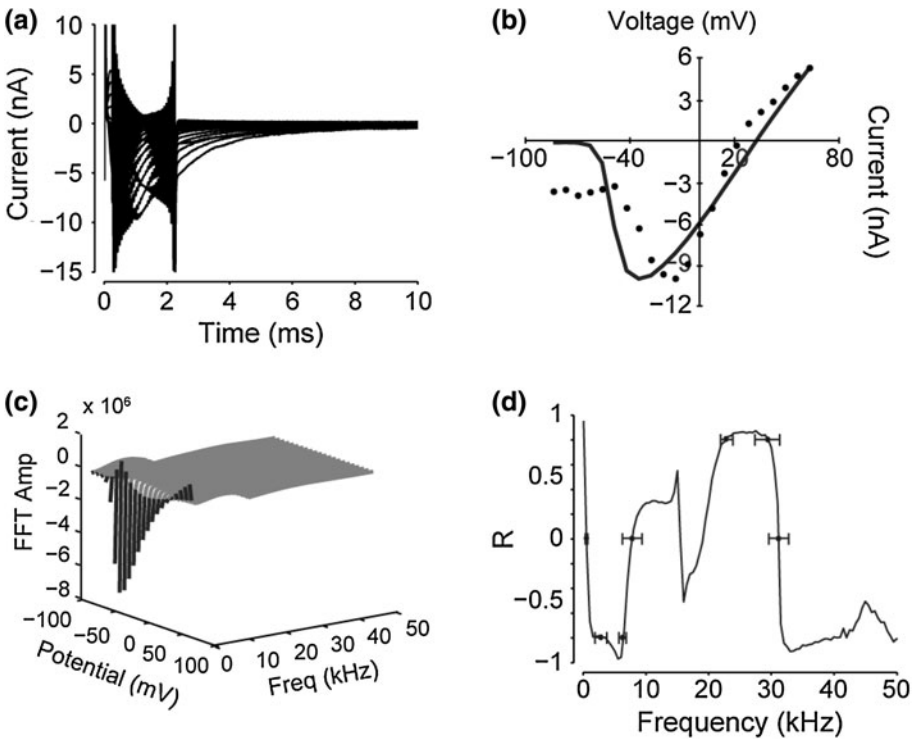

FIGURE 5. (a) Representative $Na_v1.5$ current in response to a voltage step protocol with noise function inserted. (b) Representative $Na_v1.5$ IV relationship (solid line) and the mean of all frequency magnitudes between 24.5 and 26.5 kHz for all experiments (solid circles). (c) The FFT of a 2 ms portion of each voltage step taken from the time points where the noise function was inserted. (d) Representative correlation–frequency plot comparing the IV relationship to the magnitude of individual frequencies in the FFT. Mean and standard deviation of summary data for all experiments is plotted as filled circles with bars (repeated in $n = 3$ cells).

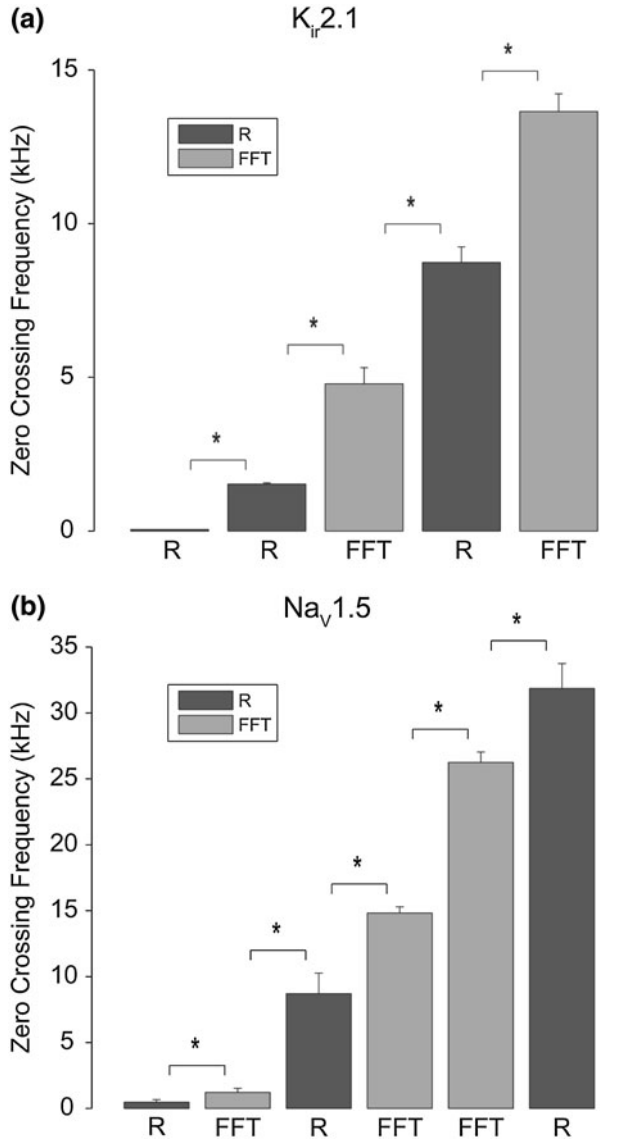

FIGURE 6. (a) Average frequency of zero FFT magnitude (FFT) and average frequency of zero correlation coefficient (*R*) for $K_{ir}2.1$ (average of $n = 6$ cells). (b) Average frequency of zero FFT magnitude and zero correlation for $Na_v1.5$ (average of $n = 3$ cells). All frequencies of zero FFT magnitude and correlation were significantly different from neighboring frequencies independent of channel type.

over each voltage step (FFT, gray bars) are presented in Fig. 6a for Kir2.1 and 6B for Nav1.5. The frequencies with correlation coefficients equal to zero are denoted as *R* (black bars) in the same figure. Importantly, frequencies with very low power were significantly different from frequencies with zero correlation suggesting that the lack of correlation is not associated with a lack of power in that portion of the spectrum. Additionally, every frequency of zero correlation was significantly different from every other frequency of zero correlation.

DISCUSSION

Previous studies using impedance spectroscopy quantified changes in the overall frequency response of membranes using the assumption that ions traverse channels with a single rate constant resulting in a constant current through each part of the channel.[11,12,19] As a result, impedance spectroscopy can determine whether the cell membrane is more or less conductive than some other state. However, impedance spectroscopy has not demonstrated which family of ion channels or even subtypes are active at a given time point of the action potential. Action potential clamping overcomes the limitation of low specificity and allows study of an individual ion channel current in an electrically active cell,[2,4] but it cannot provide simultaneous measurements of multiple ion channel types.

In this study we demonstrate that the frequency magnitude itself can correlate with the voltage-dependent current through two distinct channel families. Specifically, we present evidence that $K_{ir}2.1$ and $Na_v1.5$ exhibit unique spectra with distinct frequency magnitudes that correlate with the corresponding IV relationship. This is accomplished without making any assumptions about a cell membrane model as impedance spectroscopy requires. Therefore, this technique represents a unique variant to frequency analysis of ion channel function.

0 kHz

The DC magnitude correlates with the voltage-dependent current of both $K_{ir}2.1$ and $Na_v1.5$ (subsequently referred to as 'highly correlated'), regardless of whether a noise function was included in the step protocol ($R > 0.9$ in all cases). This is expected since most of the power in a standard whole-cell voltage clamp experiment is found within the DC component (see Figs. 1c, 2c, 3c, 4c, and 5c).[17,25]

However, the DC correlation coefficient for $K_{ir}2.1$ is notably higher than that of Nav1.5. One reason for this is likely related to the fact that $Na_v1.5$ has rapid, voltage-dependent activation and inactivation kinetics result in a peak current amplitude that is relatively stable for around 200 μs.[3,16] In order to calculate the FFT of the current trace with sufficient frequency resolution, a larger window must be used that includes additional time points on either side of the peak current. Since the kinetics are voltage-dependent, traces with more negative voltage steps (slower kinetics) will also have a mean current amplitude that is closer to the peak current amplitude over the duration of the noise function. Despite the presence of these two factors, the DC component of Nav1.5 still correlates highly with the IV relationship.

Frequencies Above DC

Under control conditions, no frequencies above DC were identified in either channel whose magnitude highly correlated ($|R| > 0.8$) with the channel's IV relationship. Upon insertion of the noise function, $K_{ir}2.1$ exhibited two frequency ranges with high correlation, both of which were under 10 kHz. These ranges of high correlation were abolished by inhibition of $K_{ir}2.1$ with $BaCl_2$, suggesting that the highly correlating frequencies were a result of the channel, and not related to the recording system. Indeed, we previously demonstrated with an artificial cell that neither the hardware nor the noise function inserted into the voltage step protocol caused the magnitude of any frequency except DC to highly correlate with the current amplitude.[23] This suggests that when a preparation containing ion channels is used, any frequency response which produces high correlations with the current amplitude is likely due to some property of the ion channel itself, and not an artifact of the equipment or protocol.

When the noise function was inserted into $Na_v1.5$, two frequency ranges were also identified which highly correlated, one of which was below 10 kHz, while the other was between 22.5 and 28.8 kHz. Importantly, both channels exhibited high correlation for frequencies below 10 kHz. Interestingly, the activation and inactivation time constants for both $K_{ir}2.1$ and $Na_v1.5$ are on the order of 100's of microseconds to 10 ms, which corresponds to a maximal frequency of activation and inactivation in a range of 0.1–10 kHz,[3,15,16,26] precisely in the high correlation range of both $K_{ir}2.1$ and $Na_v1.5$. It is possible to speculate that frequencies up to 10 kHz may be biophysically related to activation or inactivation kinetics. Impedance spectroscopy has previously been used to estimate the gating currents of voltage-dependent ion channels. In those studies, alternating currents containing frequencies between 600 and 3000 Hz were used to study channel gating kinetics and develop ion channel membrane models.[5–8] However, these studies quantified frequencies only to estimate the gating currents, but not to determine if any frequency magnitudes were uniquely correlated to the different gating currents. In the present study, the large negative correlation at 1 kHz for $K_{ir}2.1$ is associated with a zero correlation value for $Na_v1.5$ at the same frequency. The large positive correlation between 22.5 and 28.8 kHz for $Na_v1.5$ is associated with a zero correlation value for $K_{ir}2.1$ at the same frequencies. These data suggest that frequencies up to 50 kHz may be sufficient to determine differences in current amplitudes of different channel types measured simultaneously. In addition, frequencies up to 10 kHz may be sufficient to distinguish gating differences between ion channel families, if gating mechanistically underlies the correlation at these low frequencies. Further studies are needed to determine whether causality underlies correlation.

The observation that specific frequency magnitudes correlate with channel conductance has been previously suggested, but not quantified, by Terrettaz *et al.* in their Fig. 4.[27] Briefly, that figure suggests that synthetic ligand-gated ion channel impedance may be positively correlated with ligand concentration for frequencies up to approximately 1 kHz and negatively correlated with frequencies higher than 1 kHz. Importantly, impedance at approximately 1 kHz did not appear to change, regardless of ligand concentration, suggesting that the correlation at 1 kHz would be zero. However, this was not quantified. In the present study, the zero correlation frequencies were not a result of zero magnitude in the FFT (see Fig. 6).

Lastly, high correlation was observed for $Na_v1.5$ at frequencies higher than 10 kHz, but not for $K_{ir}2.1$. However, the instrumentation had a low-pass anti-aliasing filter of 50 kHz. Therefore, we were not able to assess whether $K_{ir}2.1$ or $Na_v1.5$ exhibit high correlation beyond 50 kHz. While impedance significantly decreases at high frequencies due to the capacitive nature of the cell, the presented technique is based on assessing changes in magnitude and not the absolute magnitude. Thus, higher frequency resolution may yield other new insights even if the signal to noise ratio decreases at these higher frequencies.

CONCLUSION

This study provides a novel method for relating ion channel frequency response with channel conductance. Further investigations are required to expand this technique and determine whether (1) multiple channel types can be quantified simultaneously, (2) the frequency response of various channel families and subtypes are unique, and (3) biophysical mechanisms underlie the frequency responses. Lastly, this work has important implications for understanding ion channel electrophysiology under more physiologic conditions when no channels are inhibited and the normal feedback systems between whole-cell current and voltage are preserved.

ACKNOWLEDGMENTS

This work was supported by the National Institutes of Health Grant number R21-HL094828 awarded to Dr. Poelzing.

CONFLICTS OF INTEREST

No conflicts of interest exist for any of the authors.

OPEN ACCESS

REFERENCES

[1]Abriel, H., C. Cabo, X. H. T. Wehrens, I. Rivolta, H. K. Motoike, M. Memmi, C. Napolitano, S. G. Priori, and R. S. Kass. Novel arrhythmogenic mechanism revealed by a long-QT syndrome mutation in the cardiac Na^+ channel. *Circ Res* 88:740–745, 2001.

[2]Arreola, J., R. T. Dirksen, R. C. Shieh, D. J. Williford, and S. S. Sheu. Ca^{2+} current and Ca^{2+} transients under action potential clamp in guinea pig ventricular myocytes. *Am. J. Physiol.* 261:C393–C397, 1991.

[3]Chen, T., M. Inoue, and M. F. Sheets. Reduced voltage dependence of inactivation in the SCN5A sodium channel mutation delF1617. *Am. J. Physiol. Heart Circ. Physiol.* 288:H2666–H2676, 2005.

[4]Doerr, T., R. Denger, and W. Trautwein. Calcium currents in single SA nodal cells of the rabbit heart studied with action potential clamp. *Pflugers Arch.* 413:599–603, 1989.

[5]Fohlmeister, J. F., and W. J. Adelman, Jr. Gating current harmonics. I. Sodium channel activation gating in dynamic steady states. *Biophys. J.* 48:375–390, 1985.

[6]Fohlmeister, J. F., and W. J. Adelman, Jr. Gating current harmonics. II. Model simulations of axonal gating currents. *Biophys. J.* 48:391–400, 1985.

[7]Fohlmeister, J. F., and W. J. Adelman, Jr. Gating current harmonics. III. Dynamic transients and steady states with intact sodium inactivation gating. *Biophys. J.* 50:489–502, 1986.

[8]Fohlmeister, J. F., and W. J. Adelman, Jr. Gating current harmonics. IV. Dynamic properties of secondary activation kinetics in sodium channel gating. *Biophys. J.* 51:335–338, 1987.

[9]Giles, W. R., and Y. Imaizumi. Comparison of potassium currents in rabbit atrial and ventricular cells. *J. Physiol.* 405:123–145, 1988.

[10]Hamill, O. P., A. Marty, E. Neher, B. Sakmann, and F. J. Sigworth. Improved patch-clamp techniques for high-resolution current recording from cells and cell-free membrane patches. *Pflugers Arch.* 391:85–100, 1981.

[11]Han, A., and A. B. Frazier. Ion channel characterization using single cell impedance spectroscopy. *Lab Chip* 6:1412–1414, 2006.

[12]Hayashi, H., and H. M. Fishman. Inward rectifier K^+-channel kinetics from analysis of the complex conductance of Aplysia neuronal membrane. *Biophys. J.* 53:747–757, 1988.

[13]Kargol, A., B. Smith, and M. M. Millonas. Applications of nonequilibrium response spectroscopy to the study of channel gating. Experimental design and optimization. *J. Theoret. Biol.* 218:239–258, 2002.

[14]Lee, K. S., and R. W. Tsien. Mechanism of calcium channel blockade by verapamil, D600, diltiazem and nitrendipine in single dialysed heart cells. *Nature* 302:790–794, 1983.

[15]Liu, A., M. Tang, J. Xi, L. Gao, Y. Zheng, H. Luo, X. Hu, F. Zhao, M. Reppel, J. Hescheler, and H. Liang. Functional characterization of inward rectifier potassium ion channel in murine fetal ventricular cardiomyocytes. *Cell. Physiol. Biochem.* 26:413–420, 2010.

[16]Mazzone, A., P. R. Strege, D. J. Tester, C. E. Bernard, G. Faulkner, R. De Giorgio, J. C. Makielski, V. Stanghellini, S. J. Gibbons, M. J. Ackerman, and G. Farrugia. A mutation in telethonin alters Nav1.5 function. *J. Biol. Chem.* 283:16537–16544, 2008.

[17]McGeoch, M. W., and J. E. McGeoch. Power spectra and cooperativity of a calcium-regulated cation channel. *Biophys. J.* 66:161–168, 1994.

[18]Millonas, M. M., and D. A. Hanck. Nonequilibrium response spectroscopy of voltage-sensitive ion channel gating. *Biophys. J.* 74:210–229, 1998.

[19]Misakian, M., J. J. Kasianowicz, B. Robertson, and O. Petersons. Frequency response of alternating currents through the *Staphylococcus aureus* alpha-hemolysin ion channel. *Bioelectromagnetics* 22:487–493, 2001.

[20]Owen, J. M., C. C. Quinn, R. Leach, J. B. Findlay, and M. R. Boyett. Effect of extracellular cations on the inward rectifying K^+ channels Kir2.1 and Kir3.1/Kir3.4. *Exp. Physiol.* 84:471–488, 1999.

[21]Ozdemir, S., V. Bito, P. Holemans, L. Vinet, J.-J. Mercadier, A. Varro, and K. R. Sipido. Pharmacological inhibition of Na/Ca exchange results in increased cellular Ca^{2+} load attributable to the predominance of forward mode block. *Circ. Res.* 102:1398–1405, 2008.

[22]Poelzing, S., C. Forleo, M. Samodell, L. Dudash, S. Sorrentino, M. Anaclerio, R. Troccoli, M. Iacoviello, R. Romito, P. Guida, M. Chahine, M. Pitzalis, and I. Deschenes. SCN5A polymorphism restores trafficking of a brugada syndrome mutation on a separate gene. *Circulation* 114:368–376, 2006.

[23]Rigby, J. R., and S. Poelzing. Recapitulation of an ion channel IV curve using frequency components. *J. Vis. Exp.*, 2011. doi:10.3791/2361.

[24]Rodríguez-Menchaca, A. A., R. A. Navarro-Polanco, T. Ferrer-Villada, J. Rupp, F. B. Sachse, M. Tristani-Firouzi, and J. A. Sánchez-Chapula. The molecular basis of chloroquine block of the inward rectifier Kir2.1 channel. *Proc. Natl. Acad. Sci. USA* 105:1364–1368, 2008.

[25]Sigworth, F. J. Interpreting power spectra from nonstationary membrane current fluctuations. *Biophys. J.* 35:289–300, 1981.

[26]Stanfield, P. R., N. W. Davies, P. A. Shelton, I. A. Khan, W. J. Brammar, N. B. Standen, and E. C. Conley. The intrinsic gating of inward rectifier K^+ channels expressed from the murine IRK1 gene depends on voltage, K^+ and Mg^{2+}. *J. Physiol. (Lond.)* 475:1–7, 1994.

[27]Terrettaz, S., W.-P. Ulrich, R. Guerrini, A. Verdini, and H. Vogel. Immunosensing by a synthetic ligand-gated ion channel. *Angew. Chem. Int. Ed. Engl.* 40:1740–1743, 2001.

[28]Ukomadu, C., J. Zhou, F. J. Sigworth, and W. S. Agnew. [mu]l Na^+ channels expressed transiently in human embryonic kidney cells: biochemical and biophysical properties. *Neuron* 8:663–676, 1992.

[29]Zhang, S., Z. Zhou, Q. Gong, J. C. Makielski, and C. T. January. Mechanism of block and identification of the verapamil binding domain to HERG potassium channels. *Circ. Res.* 84:989–998, 1999.